

Measurement of the differences among the charge radii of hafnium nuclei by laser resonance fluorescence

A. Ya. Anastasov, Yu. P. Gangrskii, B. N. Markov, and S. G. Zemlyanoi

Joint Institute for Nuclear Research, 141980 Dubna, Moscow Oblast, Russia

B. K. Kul'dzhanov

Institute of Nuclear Physics, Tashkent, Uzbekistan

K. P. Marinova

K. Okhridskii University, Sofia, Bulgaria

(Submitted 7 August 1993)

Zh. Eksp. Teor. Fiz. **105**, 250–259 (February 1994)

High-resolution laser spectroscopy has been used to measure the isotope shifts for optical transitions in HfI with wavelengths of 590.3 and 594.8 nm. The charge radii of Hf nuclei over the mass-number range $A=174$ – 182 have been determined. The results found are compared with calculations from the liquid-drop model. The change in the deformation of the Hf nuclei with increasing neutron number is discussed.

Research on the properties of the ground and isomer states of nuclei by laser spectroscopy has developed extensively in recent years. These methods make it possible to measure isotope shifts and hyperfine structure in optical spectra of atoms and ions on the basis of extremely small amounts of material. These results are then used to determine the nuclear moments and the differences among the charge radii in long chains of isotopes of a wide variety of elements. Our purpose in the present study was to carry out measurements of this sort for the chain of Hf isotopes in the mass-number interval $A=174$ – 182 .

The Hf isotopes are of interest because they lie at the center of the region between the filled shells of 82 and 126 neutrons. The quadrupole deformation β_2 of Hf nuclei in this region initially increases with increasing neutron number, reaches a maximum at $N=104$, and then falls off. Changes occur simultaneously in the deformation parameters of higher orders (the octupole deformation β_3 and the hexadecapole deformation β_4) and also in the amplitudes of vibrations of the nuclear surface. However, considerably less is known about these nuclear parameters. Precise measurements of the differences among charge radii and of the ratios of electric quadrupole moments by laser spectroscopy would provide detailed information on changes in the shape of Hf nuclei and on how various agents influence these changes.

Optical spectra of Hf, from which these nuclear parameters can be determined, have been measured in numerous studies. These studies have used both methods of classical interference spectroscopy^{1–3} and methods of laser spectroscopy.^{4–6} However, these measurements have either been insufficiently accurate or have covered only a comparatively narrow interval of mass numbers.

1. EXPERIMENTAL APPARATUS

The method of laser resonance fluorescence in a parallel atomic beam was used in these measurements of the

isotope shifts and hyperfine structure in the optical spectra of Hf. The experimental layout is shown in Fig. 1. The operating principle of the apparatus and certain characteristics are reported in Ref. 7. The atomic beam (selected by a system of collimators), the laser beam, and the direction at which the resonantly scattered radiation is detected are mutually orthogonal. This geometry makes it possible to carry out measurements with the highest possible resolution in terms of the frequency of the laser radiation, down to the natural width of the optical line. The atoms are excited by a tunable dye laser (Spectra Physics Model 380D) pumped by a cw argon ion laser (Spectra Physics Model 2030). The frequency of the laser radiation is automatically scanned over a selected interval up to 40 GHz wide.

The resonantly scattered radiation is focused by an optical system onto the cathode of a photomultiplier (FÉU-136) operating in the photon counting regime. The background from scattered laser radiation is reduced by detecting spontaneous emission at another wavelength, corresponding to a transition to a lower-lying state. This radiation is selected by an interference filter with a bandwidth of 15 nm positioned in front of the photomultiplier.

The time evolution of the intensity of the resonantly scattered photons, synchronized with the scanning of the laser frequency, is measured by an IBM AT286 personal computer. The laser frequency is calibrated with a Fabry–Perot interferometer in which the distance between peaks is 150 MHz. Most of the measurements were carried out by multiple scanning over the selected frequency interval. A stabilization system stabilized the initial scanning frequency within 10–20 MHz. The half-width of the resonance line increased by the same amount in the case of prolonged measurements (lasting up to several hours). This half-width was 30–50 MHz in most cases and was determined by the Doppler frequency broadening due to the finite divergence of the atomic beam. The data acquisition program blocked input during frequency excursions

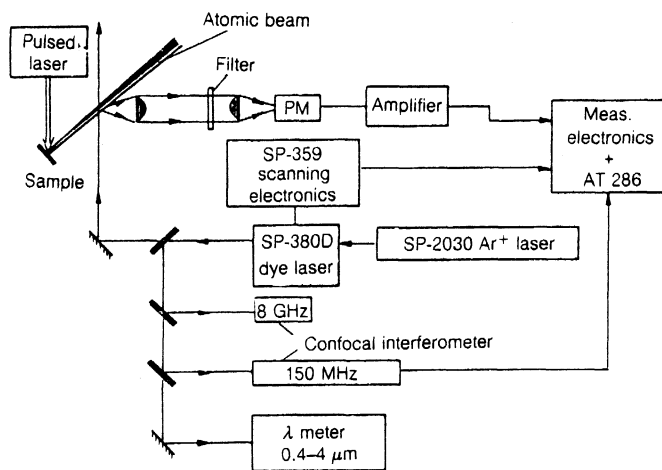


FIG. 1. Block diagram of the experimental apparatus.

of the laser radiation until the frequency was returned to its original level by the stabilization system. This measure made it possible to avoid distortions of the spectrum during malfunctions of the laser.

Hafnium belongs to the group of elements which are difficult to evaporate. In order to produce an intense atomic beam, samples were accordingly bombarded by the beam from a pulsed YAG laser (model LTIPCh-7) in *Q*-switched operation.⁸ The wavelength of this laser was 1.06 μm , its pulse length was 10 ns, the repetition rate ranged up to 100 Hz, and the power in the pulse ranged up to 5 MW. The laser radiation was focused on the target by means of a lens. The size of the light spot could be varied from 0.2 to 3 mm; the power density of the laser radiation on the target could thus be varied over a broad range. There was provision for rotating the target at a given velocity in order to increase the area of illuminated surface. Under optimum evaporation conditions, the yield was $\sim 10^{12}$ atoms per laser pulse, with free atoms amounting to $\sim 10\%$ in the case of both metallic hafnium and its oxide.⁹

The pulses from the photomultiplier were detected in synchronism with the operation of the evaporating laser: The resonantly scattered photons were counted only at the time at which a bunch of atoms passed through the scanned laser radiation. This approach made it possible to reduce the background to 10–20 counts/s.

The efficiency of the apparatus was such that one pulse

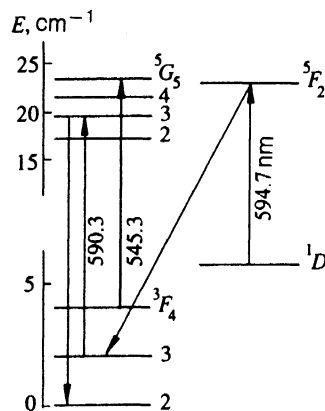


FIG. 2. Level scheme of Hf atoms. The arrows show the transitions used in the measurements.

from the photomultiplier corresponded to $\sim 10^8$ atoms emitted from the target. This efficiency incorporates the loss of atoms due to the collimation, the relative number of atoms in a definite quantum state and in the Doppler contour within the width of the laser line, and also the photon detection efficiency of the photomultiplier.

2. EXPERIMENTAL RESULTS

Three types of samples were used in measuring the Hf optical spectra:

- 1) a plate of metallic hafnium with the natural isotopic composition;
- 2) pressed tablets of oxides (HfO_2) of the separated isotopes ^{177}Hf and ^{179}Hf ;
- 3) a plate of metallic tungsten which had been bombarded by bremsstrahlung with a maximum energy of 25 MeV. In the latter case, the plate had served as the bremsstrahlung target of a microtron for several years. In it, the (γ, α) reaction at W isotopes resulted in the production of Hf isotopes with $A=178, 179, 180,$ and 182 , all in amounts $\sim 10^{15}$ nuclei. The last of these isotopes (^{182}Hf) is radioactive (with a half-life of $9 \cdot 10^6$ yr). It has never previously been used in optical measurements. The Hf isotopes produced in the (γ, α) reaction were distributed uniformly over the entire thickness (3 mm) of the tungsten target.

TABLE I. Characteristics of optical transitions of Hf atoms.

λ_1, nm	λ_2, nm	E, cm^{-1}	Term	Configuration
590.3	518.2	2366→19293→0	$a^3F_3 \rightarrow z^5G_3 \rightarrow a^3F_2$	$5d^26s^2 \rightarrow 5d^26s6p + (5d6s^26p)$
594.7	497.8	5639→22451→2357	$a^1D_2 \rightarrow z^5F_2 \rightarrow a^3F_3$	$5d^26s^2 \rightarrow 5d^26s6p$

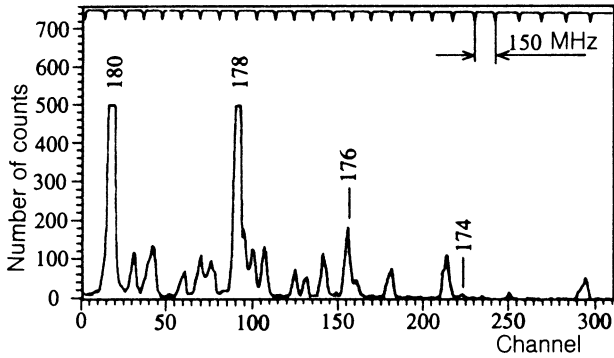


FIG. 3. Resonance fluorescence spectrum of Hf atoms from a sample of natural isotopic composition. The peaks are labeled with the isotope mass numbers.

For the measurements we used only a surface layer of the target (3–5 μm thick), containing $\sim 10^{12}$ atoms of ^{180}Hf or ^{182}Hf .

The Hf atoms have a complex level spectrum.¹⁰ Figure 2 shows part of the scheme of excited states, including the multiplets of levels used in the measurements and transitions between them. For the measurements we selected two transitions with fairly large negative field shifts. Their characteristics (energies; terms; and configurations of the initial, excited, and final levels; and wavelengths of the excited radiation, λ_1 , and of the detected radiation, λ_2) are listed in Table I. Although these transitions have small oscillator strengths, the intensities of the laser radiation used in these experiments (up to 150 mW) resulted in a fairly high yield of resonance fluorescence.

Figures 3–5 show examples of the measured resonance fluorescence spectra of Hf atoms. For a sample of metallic Hf with the natural isotopic composition, we see peaks corresponding to all the even-even isotopes and certain components of the hyperfine structure of odd isotopes (Fig. 3). All the components of the hyperfine structure are seen when we use samples of the separated ^{177}Hf and ^{179}Hf isotopes (Fig. 4). From the center of gravity of the components of the hyperfine structure we can determine the

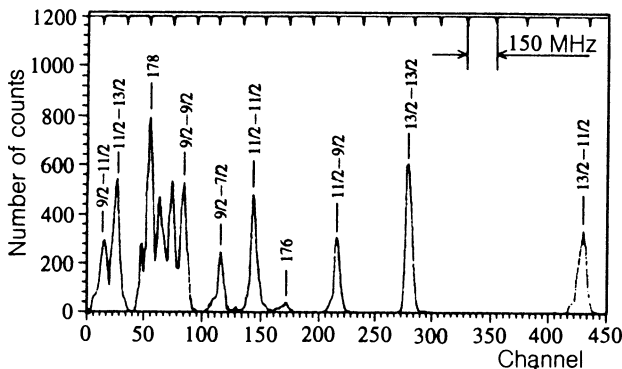


FIG. 4. Hyperfine structure in the optical spectrum of ^{177}Hf . The peaks are labeled with the spins of the components of the upper and lower levels.

isotopic shifts of the odd isotopes with respect to the neighboring even-even isotopes. In the resonance fluorescence spectrum of a sample of metallic tungsten (the bremsstrahlung target of the microtron) we identified peaks belonging to the isotopes ^{180}Hf and ^{182}Hf (Fig. 5).

Table II shows isotope shifts for the two optical transitions studied. The small linewidth (~ 45 MHz), the large statistical base of events, and the good reproducibility of results made it possible to keep the errors in the differences between resonant frequencies smaller than in all previous measurements (as small as 0.2%).

3. ANALYSIS OF RESULTS

To find the differences in the mean square charge radii of the Hf nuclei, $\Delta\langle r^2 \rangle$, we used the method of Ref. 11 to process the measured values of the isotope shifts. In that method, the difference between resonance frequencies, after corrections for the normal and specific mass shifts, is related to the difference between charge radii by

$$\Delta\nu^{A,A'} = E_i f(Z) \lambda^{A,A'}, \quad (1)$$

$$\lambda^{A,A'} = \Delta\langle r^2 \rangle^{A,A'} + \frac{C_2}{C_i} \Delta\langle r^4 \rangle^{A,A'} + \frac{C_3}{C_i} \Delta\langle r^6 \rangle^{A,A'} + \dots, \quad (2)$$

where E_i and $f(Z)$ are, respectively, electron and nuclear factors, and the C_i reflect the contributions of the moments of various orders to the radial profile of the electric charge of the nucleus. This contribution is essentially independent of the principal quantum number of the electron shell, so it is the same for optical and x-ray transitions. When we used values of C_i calculated for the $2p \rightarrow 1s$ transitions and a Fermi charge distribution in the nucleus,¹² this contribution amounted to 5% in the case of Hf isotopes.

The normal mass shift is calculated from

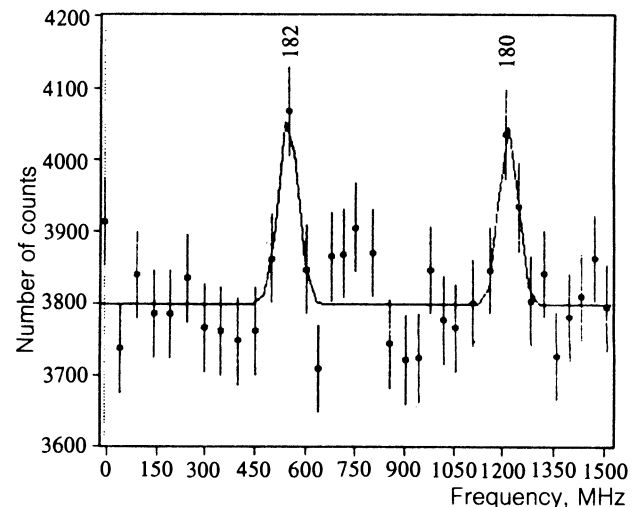


FIG. 5. Spectrum of the resonance fluorescence of Hf atoms from a tungsten bremsstrahlung target. The peak labels are the isotope mass numbers.

TABLE II. Isotope shifts in optical spectra of Hf.

A	A'	$\Delta\nu^{A,A'}$, MHz	
		$\lambda = 590.3$ nm	$\lambda = 594.7$ nm
174	176	-846.4(2,1)	-1082.4(11,2)
176	178	-862.0(1,8)	-1097.4(3,0)
177	178	-614.8(0,8)	-772(23)
178	179	-370.1(4,1)	-483(18)
178	180	-989.3(3,2)	-1260.5(1,9)
180	182	-680.0(12,7)	

$$\Delta\nu_{nms}^{A,A'} = 5.487 \cdot 10^{-4} \nu_i \frac{A-A'}{AA'}, \quad (3)$$

where ν_i is the frequency of the atomic transition in megahertz. For both transitions, the values of $\Delta\nu_{nms}$ are considerably smaller than the measured isotope shifts (Table III) and amount to merely a small correction.

Determining the specific mass shift $\Delta\nu_{sms}$ and the electron factor E_i is a more complicated problem, since neither of the transitions used in these experiments is a pure $ns \rightarrow np$ transition, and the admixtures of other configurations are unknown. Values of $\Delta\nu_{sms}$ and E_i were accordingly determined through a comparison with the corresponding values for pure transitions with the help of a King plot.¹³ The coordinates in this plot are modified isotope shifts ξ_i for the line under study and for the pure transition for several pairs of isotopes:

$$\xi_i = \Delta\nu_i^{A,A'} \frac{AA'}{A-A'}. \quad (4)$$

The slope of this straight line gives us the ratio of the electron factors for the two transitions, and the intersection of the line with the x axis gives us the specific mass shift.

Analysis of the level spectra of the Hf atoms^{1,14} shows that the transition with $\lambda = 545.3$ nm between the 3F_4 and 5G_5 levels can be regarded as a pure $ns^2 \rightarrow nsnp$ transition (Fig. 2). For this transition we have $\Delta\nu_{sms} = (0 \pm 0.5)\Delta\nu_{nms}$, and the electron factor calculated by the Goudsmit-Fermi-Segré method¹⁵ and the experimental data from Ref. 16 is 0.454(27).

The isotope shifts known for this transition^{1,14} made it possible to find values of $\Delta\nu_{sms}$ and E_i for the transitions used in these experiments with the help of a King plot. These characteristics of the transitions are shown in Table III. The values of $\Delta\nu_{sms}$ and E_i found by this method, along

with the nuclear factor¹⁷ $f(Z) = 39.908$ GHz/fm², made it possible to determine the relative values λ_{rel} and the absolute values $\Delta\langle r^2 \rangle$ of the differences between the charge radii of the Hf nuclei in the mass-number interval $A = 174-182$ (Table IV) from the measured isotope shifts.

The errors in relative measurements of the differences between charge radii, λ_{rel} , are determined exclusively by the errors in the measurement of the difference $\Delta\nu$ between resonance frequencies; they are quite small (0.2-0.3%). The errors in the absolute values of $\Delta\langle r^2 \rangle$, in contrast, include the uncertainties in the isotope-shift parameters $\Delta\nu_{sms}$ and E_i and are therefore considerably larger (5-7%).

The results we found agree well with the results of some other studies,¹⁻⁶ in which values of $\Delta\langle r^2 \rangle$ were determined from measured values of the isotope shifts in optical spectra, generally by different methods. On the other hand, our values are considerably smaller (by ~30%) than the values found for $\Delta\langle r^2 \rangle$ from measurements of the spectra of K x-rays¹⁸ or mesic atoms.¹⁹ For the pair of isotopes $^{178}\text{Hf}-^{180}\text{Hf}$, for example, the values found for $\Delta\langle r^2 \rangle$ in those studies were 0.103(7) and 0.106(7) fm², respectively.

The changes in the charge radii when one neutron beyond a neutron pair is added are usually characterized by the even-odd difference parameter

$$\gamma = \frac{\Delta\langle r^2 \rangle^{N,N+1}}{\frac{1}{2}\Delta\langle r^2 \rangle^{N,N+2}}. \quad (5)$$

In the case of the isotopes ^{177}Hf and ^{179}Hf , the values of γ are 0.277(4) and 0.338(6), respectively; these are typical values for nuclei in this region.

TABLE III. Parameters of isotope shifts in optical spectra of Hf atoms ($A=178$, $A'=180$).

λ , nm	$\Delta\nu_{nms}$, MHz	$\Delta\nu_{sms}$, MHz	E_i
545.3	18.8	0.0(9,4)	-0.454(27)
590.3	17.3	-112(28)	-0.313(21)
594.8	17.2	-153(80)	-0.395(38)

TABLE IV. Differences between the charge radii of Hf nuclei.

A	$\lambda_{rel}^{178,A}$	$\Delta\langle r^2 \rangle^{178,A}, \text{fm}^2$
174	-1.698(5)	-0.126(6)
176	-0.853(3)	-0.063(3)
177	-0.617(3)	-0.046(3)
179	0.338(6)	0.024(2)
180	1.00	0.075(4)
182	1.656(62)	0.124(8)

The distance between the components of the hyperfine structure in odd isotopes of Hf can be used to determine the magnetic dipole and electric quadrupole moments.

4. DISCUSSION OF RESULTS

Figure 6 shows the change in the charge radius resulting from the addition of a neutron pair, $\Delta\langle r^2 \rangle^{N,N+2}$, versus the number of neutrons in the nucleus. To the values found for $\Delta\langle r^2 \rangle^{N,N+2}$ in the present study we have added the corresponding value for the isotope pair ^{172}Hf - ^{174}Hf from Ref. 20. We see that the difference in charge radii decreases with increasing number of neutrons in the nucleus in this range of mass numbers. This change in charge radius is characteristic²¹ of isotopes which are neighbors of Hf (Yb,Er).

The liquid-drop model is ordinarily used to describe the behavior of charge radii over wide ranges of the mass number.^{22,23} According to that model, the change in charge radius is determined by the sum of two terms:

$$\Delta\langle r^2 \rangle^{N,N'} = \Delta\langle r^2 \rangle_v^{N,N'} + \Delta\langle r^2 \rangle_\beta^{N,N'} \quad (6)$$

The first term in this expression stems from the change in the volume of a nucleus due to an increase in the number of neutrons in it. For the parameters of nuclei differing by two neutrons which are adopted in the liquid-drop model, the value of this term is $\Delta\langle r^2 \rangle_v^{N,N'+2} = 0.12 \text{ fm}^2$.

The second term is determined by the change in the deformation of the nucleus:

$$\Delta\langle r^2 \rangle_\beta^{N,N'} = \frac{5}{4\pi} \langle \bar{r}^2 \rangle_0 \sum_i \Delta\langle \beta_i^2 \rangle, \quad (7)$$

where $\langle \bar{r}^2 \rangle_0$ is the mean square charge radius of a spherical nucleus of the same volume (the average value for nuclei with neutron numbers N and N'), and β_i is the deformation parameter of order i . The quantity $\Delta\langle r^2 \rangle_\beta$ is a fairly strong function of the deformation parameter. For nuclei in the Hf region, for example, a change in β_2 (the quadrupole-deformation parameter) from 0.20 to 0.25 is accompanied by an increase of 0.25 fm^2 in the charge radius, i.e., by an increase much larger than that found when a pair of neutrons are added.

In the Hf isotopes studied, the quadrupole deformation is predominant. Figure 6 shows experimental values of β_2 versus the neutron number in the nucleus.²⁴ Up to $N=104$ (^{176}Hf), the quadrupole deformation increases, so we have $\Delta\langle r^2 \rangle^{N,N+2} > 0$. The deformation then begins to decrease, and the value of $\Delta\langle r^2 \rangle^{N,N+2}$ goes negative. The changes in β_2 are fairly large (~ 0.01), so the two terms in expression (6), $\Delta\langle r^2 \rangle_v$ and $\Delta\langle r^2 \rangle_\beta$, are comparable in magnitude. As a result, the characteristic slope of $\Delta\langle r^2 \rangle^{N,N+2}$ vs the neutron number in the nucleus calculated from the liquid-drop model should change at $N=104$, where β_2 reaches a maximum (Fig. 6). Experimentally, in contrast, the dependence is much smoother, and the value of $\Delta\langle r^2 \rangle^{N,N+2}$ and $N < 104$ is considerably smaller than the theoretical values.

To explain this discrepancy between experimental and theoretical behavior we must obviously incorporate other effects which would influence the charge radius of nuclei and offset the decrease in quadrupole deformation. Such effects might be higher-order deformations: octupole, β_3 , and hexadecapole, β_4 . However, the values of β_3 and β_4 cannot be measured nearly as accurately as β_2 . The octupole deformation parameters are known only within an error of at least 15–20%, and they tend to decrease with increasing N (Ref. 25). The values of β_3 are small (< 0.1), and their incorporation would apparently not improve the agreement with experiment.

The accuracy of the experimental values of the hexadecapole-deformation parameters is even worse.^{26,27} At the same time, it follows from theoretical calculations of the nuclear shape^{28,29} and the systematics of the deformation parameters that β_4 would be a strong function of

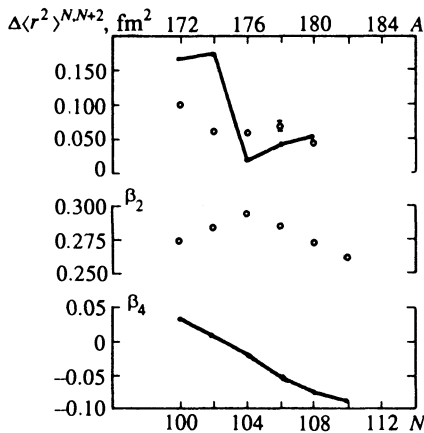


FIG. 6. Difference between the charge radii and parameters of the quadrupole and hexadecapole deformations versus the neutron number. Points—Experimental data; lines—theoretical.

the number of neutrons in the nucleus (Fig. 6). The change in β_4 is in the direction opposite that of β_2 : In the region in which β_2 increases ($N < 104$), the value of $\beta_4 > 0$ decreases in magnitude; in the region in which β_2 decreases ($N > 104$), we have $\beta_4 < 0$, and this parameter increases in absolute value. This behavior of the hexadecapole deformation weakens the effect of the quadrupole deformation on the charge radius of the nucleus. Although the values of β_4 and their changes are considerably larger than for β_3 , they are still too small to reconcile the theoretical and experimental results on the behavior of $\Delta\langle r^2 \rangle$ as a function of N . The apparent explanation is either that the actual values of β_4 are higher than the theoretical values (this possibility does not contradict experimental data²⁷), or we need to take account of yet other effects which would influence the charge radius, e.g., the thickness of a surface layer of the nucleus.

We wish to thank Yu. Ts. Oganessian and Yu. É. Penionzhkevich for constant interest in this study. We also thank V. E. Zhuchko, P. Zuzaan, and L. M. Mel'nikova for assistance in the measurements and in the analysis of the results.

- ¹J. Caiko, *Z. Phys.* **234**, 443 (1970).
²P. Aufmuth, R. Kirsch, A. Steudel, and E. Wöbker, *Z. Phys. D* **7**, 153 (1987).
³P. Aufmuth, I. Henneberg, A. Siminski, and A. Steudel, *Z. Phys. D* **18**, 107 (1991).
⁴A. Werner and D. Zimmermann, *Hyperfine Interact.* **9**, 197 (1981).
⁵D. Zimmermann, A. Werner, and A. Nunnemann, *Nucl. Sci. Res. Conf., Ser. 3*, 287 (1982).
⁶J. Schekker, A. Berges, J. Das *et al.*, *Phys. Rev. A* **46**, 3730 (1992).

- ⁷Yu. P. Gangrskii, K. P. Marinova, B. N. Markov *et al.*, *Izv. Akad. Nauk SSSR, Ser. Fiz.* **49**, 2261 (1985).
⁸Yu. P. Gangrskii, S. G. Zemlyanov, I. N. Izosimov *et al.*, *Prib. Tekh. Eksp.*, No. 1, 168 (1990).
⁹A. Ya. Anastassov, Yu. P. Gangrskii, K. P. Marinova *et al.*, *Working Conference on Laser Applications in Nuclear Physics*, Dubna, 1990, p. 17.
¹⁰C. E. Moore, *Atomic Energy Levels III*, National Bureau of Standards, Washington, 1958.
¹¹K. Heulig and A. Steudel, *At. Data Nucl. Data Tables* **14**, 613 (1974).
¹²E. C. Seltzer, *Phys. Rev.* **188**, 1916 (1969).
¹³W. H. King, *J. Opt. Soc. Am.* **53**, 638 (1963).
¹⁴P. Bauman, D. Kuszner, A. Nunnemann *et al.*, *The Second European Conf. on Atomic and Molecular Physics, Abstract MO-13*, Amsterdam, 1985.
¹⁵H. G. Kuhn, *Atomic Spectra*, Longmans, London, 1969.
¹⁶E. Finckh and A. Steudel, *Z. Phys.* **141**, 19 (1955).
¹⁷D. Zimmermann, *Z. Phys. A* **321**, 23 (1985).
¹⁸F. Boehm and P. L. Lee, *At. Data Nucl. Data Tables* **14**, 605 (1974).
¹⁹Y. Tanaka, R. M. Steffen, E. B. Shera *et al.*, *Phys. Rev. C* **30**, 350 (1984).
²⁰J. Rink, B. Gorski, W. Kälber *et al.*, *Z. Phys. A* **342**, 488 (1992).
²¹P. Aufmuth, K. Heulig, and A. Steudel, *At. Data Nucl. Data Tables* **37**, 455 (1987).
²²W. D. Myers, *Droplet Model of the Nucleus*, IFI Plenum, New York, 1977.
²³W. D. Myers and K. Schmidt, *Nucl. Phys. A* **410**, 61 (1983).
²⁴S. Raman, C. H. Malarkey, W. T. Milner *et al.*, *At. Data Nucl. Data Tables* **36**, 1 (1987).
²⁵R. H. Spear, *At. Data Nucl. Data Tables* **48**, 55 (1989).
²⁶D. L. Hendrie, N. K. Glendening, B. G. Harvey *et al.*, *Phys. Lett. B* **26**, 127 (1968).
²⁷R. M. Ronningen, J. H. Hamilton, L. Varnvell *et al.*, *Phys. Rev. C* **16**, 2208 (1977).
²⁸P. Möller and R. Nix, *At. Data Nucl. Data Tables* **26**, 165 (1981).
²⁹B. Nerlo-Pomorska, K. Pomorski, M. Brack *et al.*, *Nucl. Phys. A* **462**, 252 (1987).

Translated by D. Parsons